

Gamma-ray burst observations with the CALET Gamma-ray Burst Monitor

Yuta Kawakubo for the CALET collaboration

Dept. of Physics & Astronomy, Louisiana State University, Baton Rouge, LA, 70803

Summary: The CALET Gamma-ray Burst Monitor (CGBM) is a scintillation detector to observe gamma-ray bursts (GRBs). The CGBM is mounted in the CALorimetric Electron Telescope (CALET) on the International Space Station (ISS). The CGBM can observe GRB light curves and spectra in the energy range of 7 keV to 20 MeV due to two kinds of scintillation detectors the Hard X-ray Monitor (HXM) and the Soft Gamma-ray Monitor (SGM). As of late June 2019, CGBM has detected 161 GRBs since October 2015. The durations of the CGBM-detected GRBs were measured by the SGM in the 40 ~ 1000 keV energy band. As a result, 19 out of 161 GRBs were short bursts which are primary candidates of the electromagnetic counterparts of gravitational wave sources. We performed spectral analysis for 4 bright, short GRBs out of 19 to compare the spectral parameters with those of GRB 170817A. Although observed fluxes of the 4 GRB in the 30 ~ 1000 keV range were more than ~ 10 times as large as GRB 170817A, E_{peak} of GRB 180703B was comparable with GRB 170817A.

CALET Gamma ray Burst Monitor (CGBM)

CGBM is a secondary instrument on the CALorimetric Electron Telescope (CALET) [1][2].

Hard X-ray Monitor (HXM) Soft Gamma-ray Monitor (SGM)

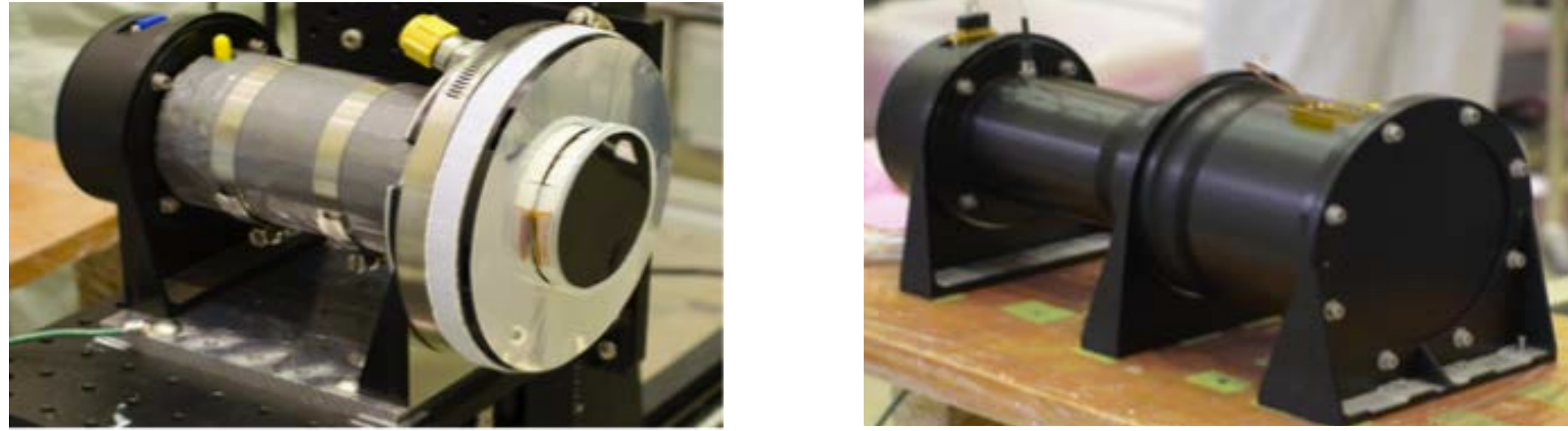


Figure 1. Pictures of the HXM and SGM. SGM is BGO covered by a housing made of aluminum, HXM is LaBr₃(Ce) with a Be window to detect low energy X-rays.

Table 1. CGBM characteristics

	HXM	SGM
Crystal	LaBr ₃ (Ce)	BGO
Number of detectors	2	1
Diameter [mm]	66.1 (small) 78.7 (large)	102
Thickness [mm]	12.7	76
Energy range [keV]	7-1000	40-20000
Field of view	~3 sr	~8 sr

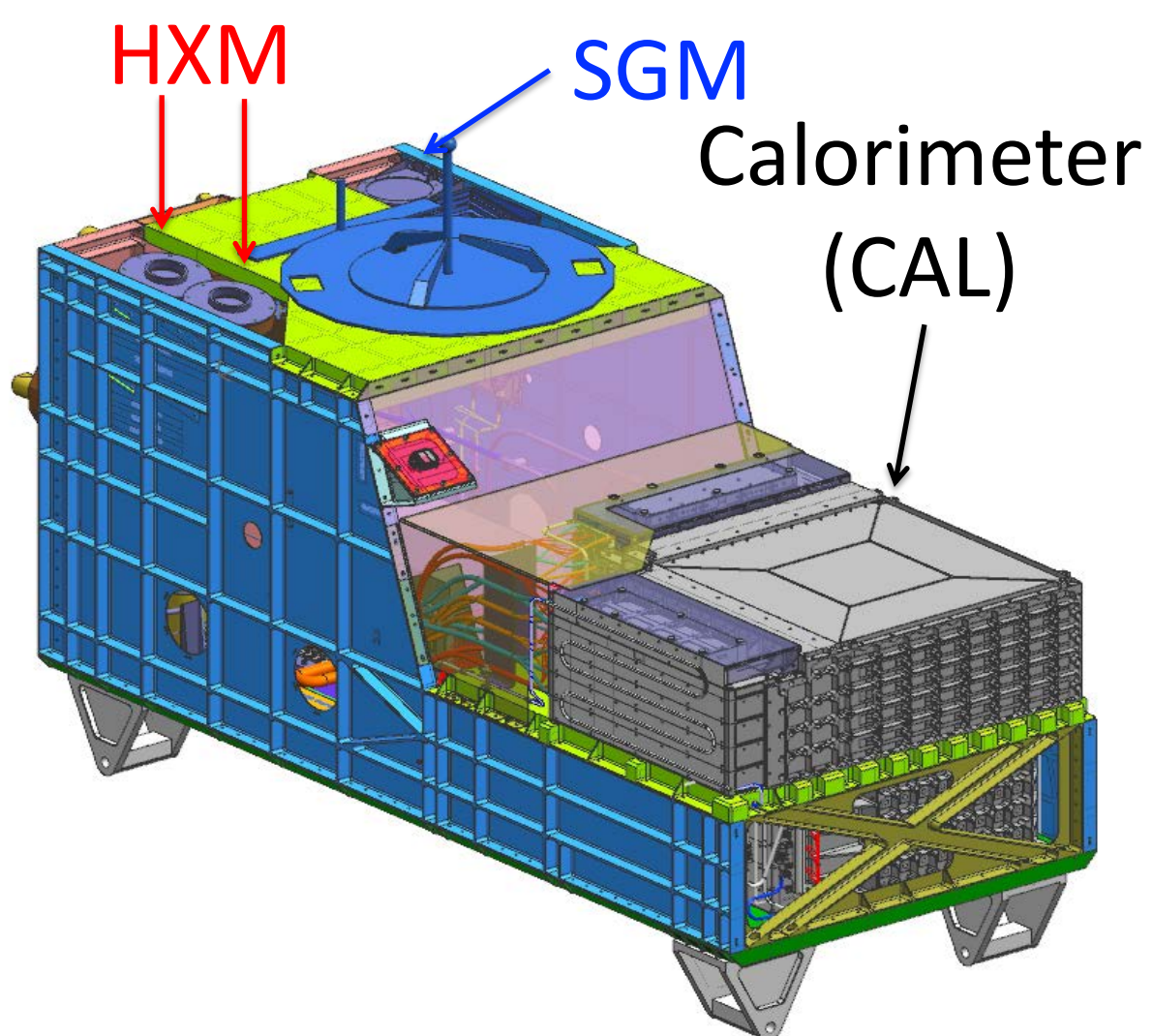


Figure 2. Schematic image of the CALET. The two HXMs and SGM are mounted on the upper side of the CALET. CAL is a main high energy calorimeter.

CGBM consists of two HXMs and one SGM. Both HXM and SGM are scintillation detectors, LaBr₃(Ce) and BGO, respectively. CGBM collects light curve data and spectral data for each 1/8 s and 4 s, respectively. If CGBM detects a transient, CGBM captures event data (62.5 us, 4096 x 2 energy channels).

Thanks to the two crystals, CGBM covers the 7 keV – 20 MeV energy range.

GRB observation with CGBM

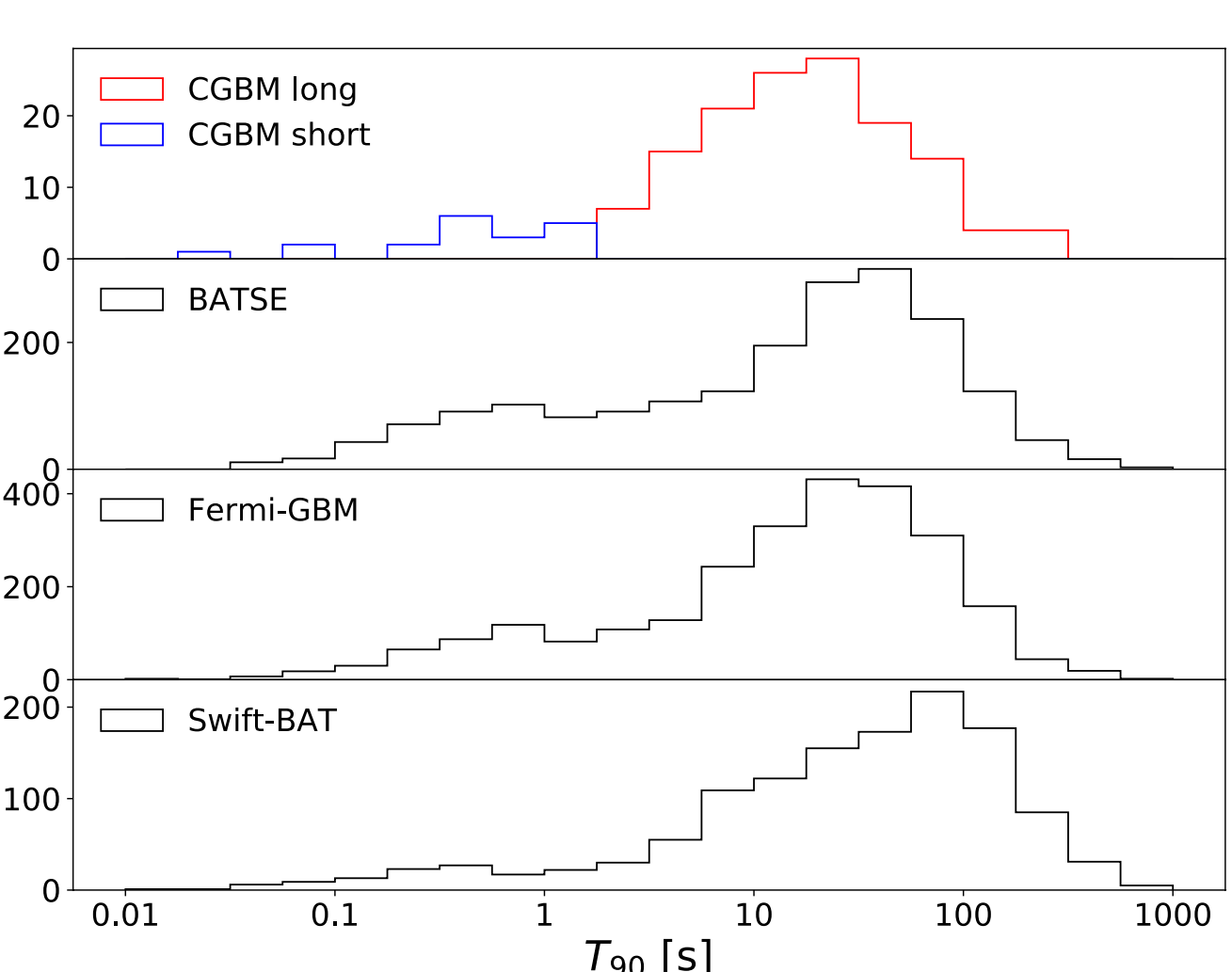


Figure 3. Duration distribution of GRBs.

CGBM has detected 161 GRBs since October 2015 with ~ 60 % duty cycle. The detection rate is 43 GRBs per year. The distribution of duration (T_{90}) is bimodal in a log scale. The number of short GRBs is 19, which corresponds to 12 % of the CGBM GRB sample.

CGBM can detect short GRBs, primary candidates for the counterparts of gravitational wave sources.

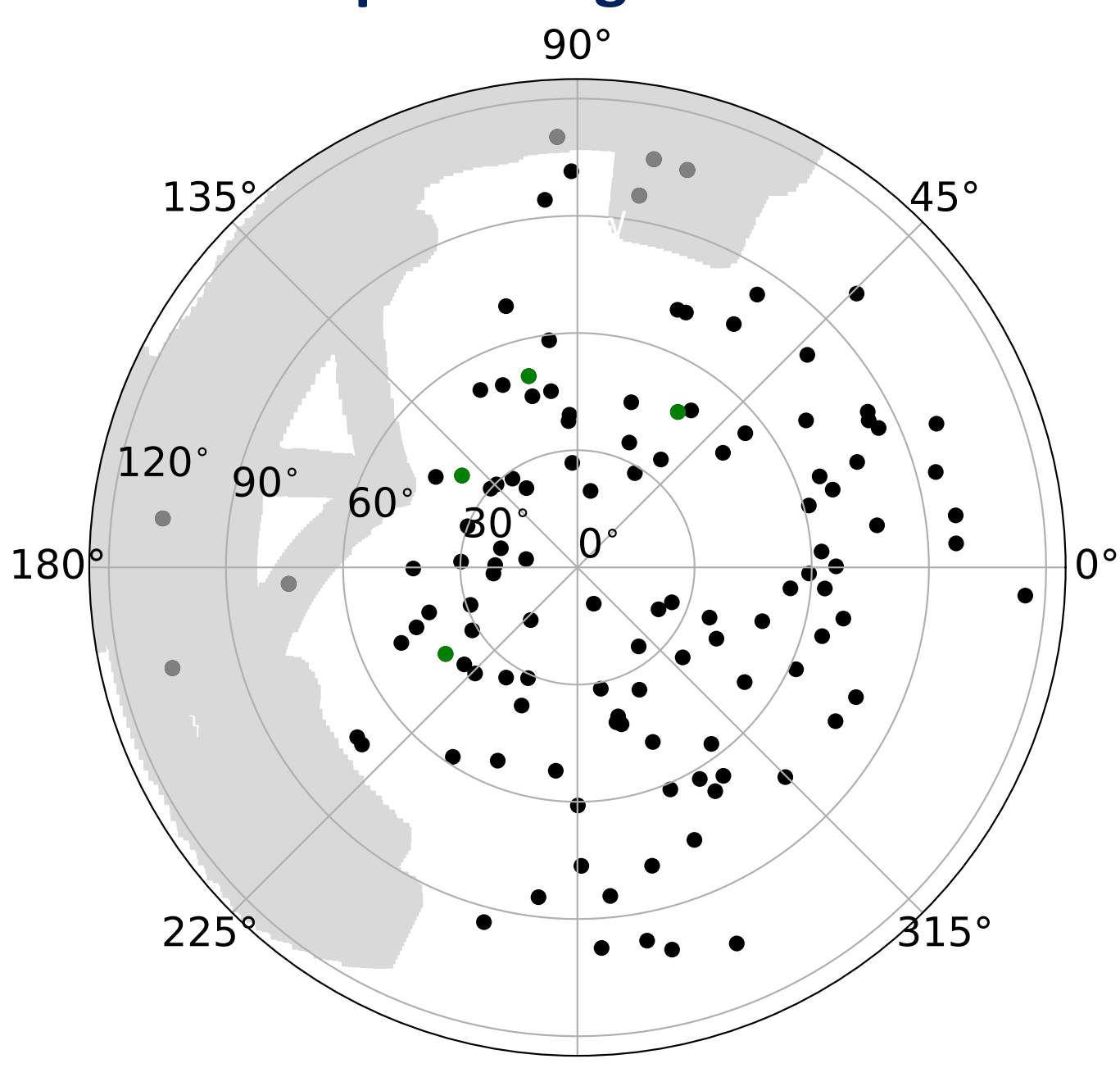


Figure 4. Incident angle distribution of CGBM-detected GRBs within the CGBM FOV. ISS structures block part of the CGBM field of view (gray). 4 GRBs for which spectra are analyzed in this paper are shown as green.

After account is taken of the ISS structures blocking part of the CGBM field of view, CGBM monitors the X-ray and gamma-ray sky.

Light curve and spectra of bright short GRBs

Short GRBs are primary candidates for counterparts of gravitational wave sources. GRB 170817A is the only short GRB associated with a binary neutron star merger event [3][4]. Since LIGO and Virgo began the third observation run in April 2019, the importance of simultaneous observation of short GRBs has increased.

We performed spectral analysis for 4 short GRBs which have enough statistics and came from known direction, to compare spectral parameters with those of GRB 170817A.

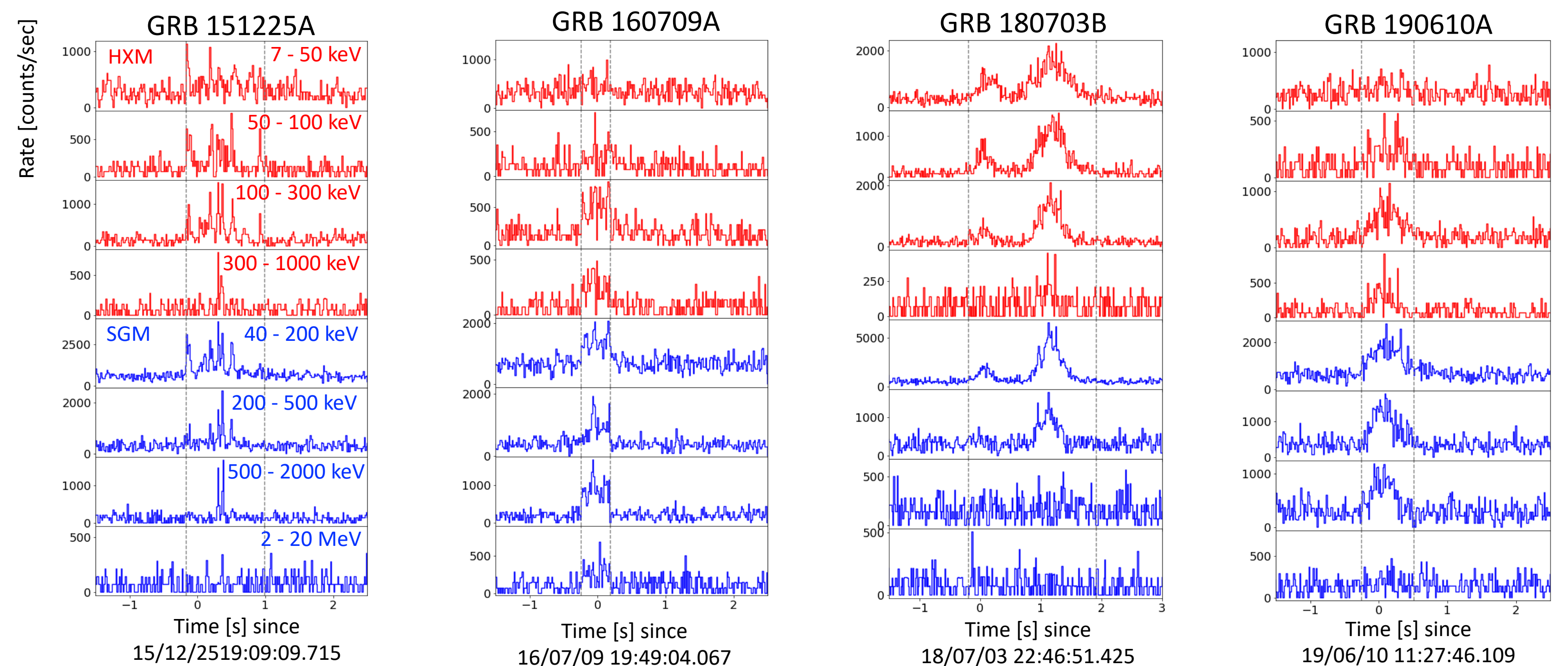


Figure 5. Light curves of four bright short GRBs detected by CGBM. Spectra were produced from T_{100} shown as dashed gray lines.

Spectra of 4 GRBs are fitted by a cutoff power-law model $N(E) = A \left(\frac{E}{200 \text{ keV}} \right)^\alpha \exp \left[-\frac{E(2+\alpha)}{E_{\text{peak}}} \right]$, where A is normalization at 200 keV, α is photon index, and E_{peak} is peak energy of the νF_ν spectrum. CGBM tends to observe spectra of GRBs, which is consistent with a Band function [5] at low energy. As a result, spectra are well fitted by the cutoff power-law. Spectral intervals are T_{100} of the bursts. Background spectra are produced from the data before and after the burst duration.

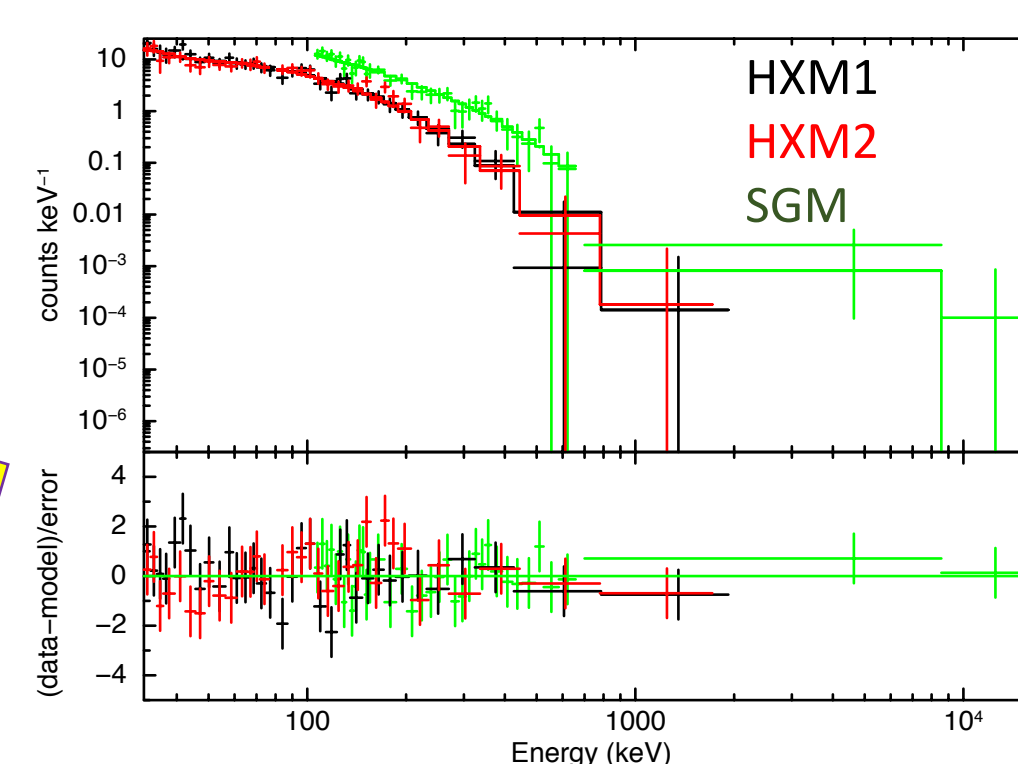


Figure 6. Spectra of GRB 180703B. Solid lines show optimized cutoff power-law model.

Table 2. Derived spectral parameters of four short GRBs

GRB	α	E_{peak} [keV]	Flux (30-1000 keV) [erg cm ⁻² s ⁻¹]	$\chi^2 / \text{d.o.f}$	Null prob.
151225A	-1.1 ± 0.3	431 (-99 / +167)	$(2.8 \pm 0.2) \times 10^{-6}$	57.82 / 55	0.372
160709A	-0.5 ± 0.2	2053 (-325 / +428)	$(6.9 \pm 0.5) \times 10^{-6}$	42.39 / 38	0.287
180703B	-1.2 ± 0.2	146 (-17 / +18)	$(3.3 \pm 0.1) \times 10^{-6}$	83.41 / 110	0.972
190610A	-0.5 ± 0.3	792 (-126 / +174)	$(5.8 \pm 0.4) \times 10^{-6}$	59.11 / 57	0.398

- Spectra of the 4 GRBs are consistent with a cutoff power-law model.
- Derived spectral parameters are consistent with the expectation of synchrotron shock model [6].

The distribution of energy flux vs. E_{peak}

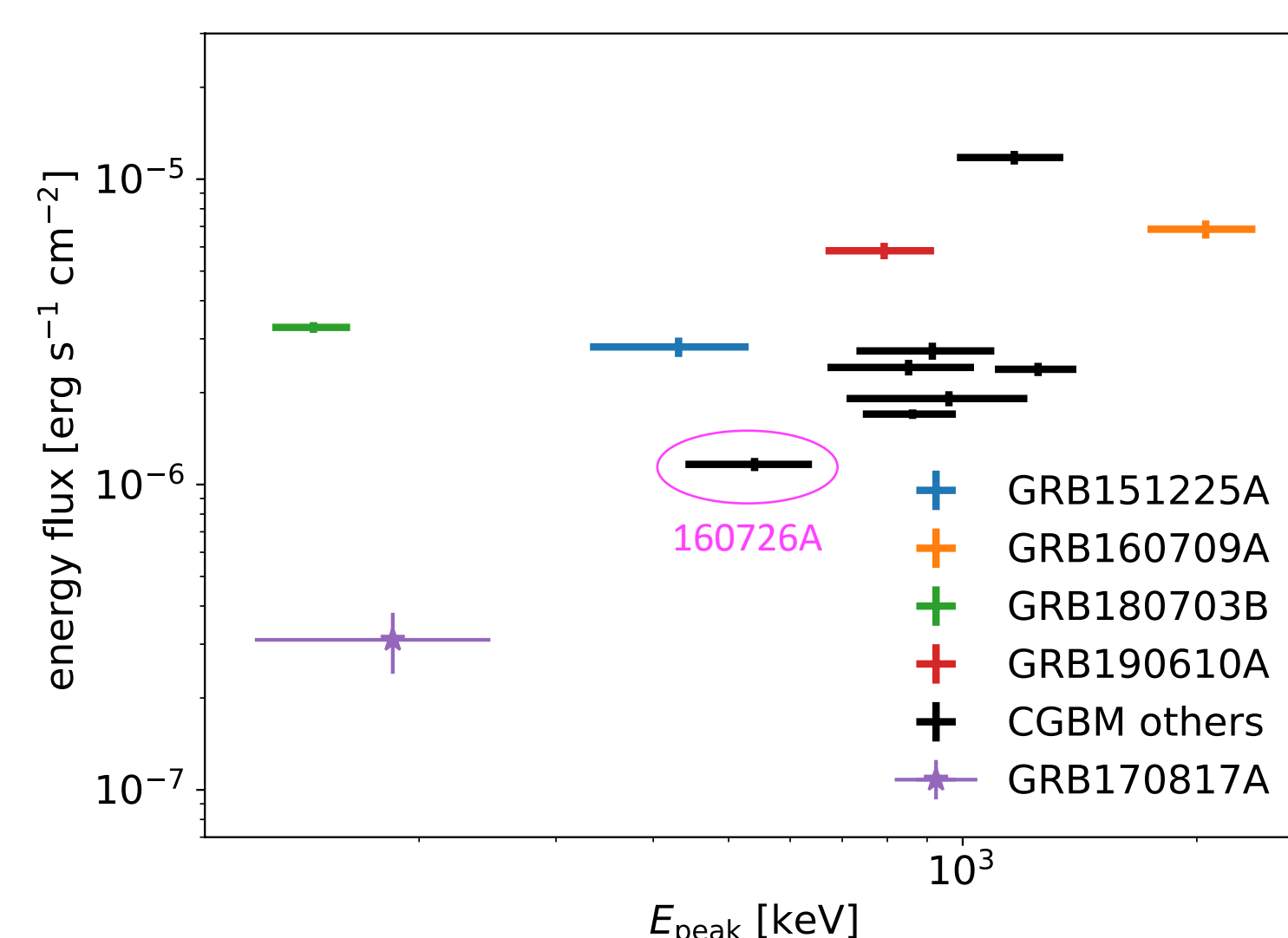


Figure 7. Distribution of energy flux (30-1000 keV) vs. E_{peak} . The flux of GRB 170817A is much less than those of CGBM-detected GRBs.

- The energy flux of GRB 170817A was more than ~ 10 times as small as those of the four bright, short GRBs for which CGBM can measure spectral parameters.
- CGBM detected GRB 160726A of which flux was ~ 4 times as large as that of GRB 170817A.
- CGBM can detect a GRB for which E_{peak} is comparable with that of GRB 170817A

Future work

Although no high energy gamma-rays from GRBs have been detected by CAL so far, count rates of the Charge detector (CHD) and Imaging calorimeter (IMC) of the CAL increased around some GRBs detected by CGBM. CHD and IMC can detect signal caused by short GRBs even if CGBM data are not available due to the ~60 % duty cycle. We will investigate the feasibility of GRB detection by CHD and IMC. Also, we are trying to extract spectral information from CHD and IMC count rates. More detail is described in Cannady et al. [9].

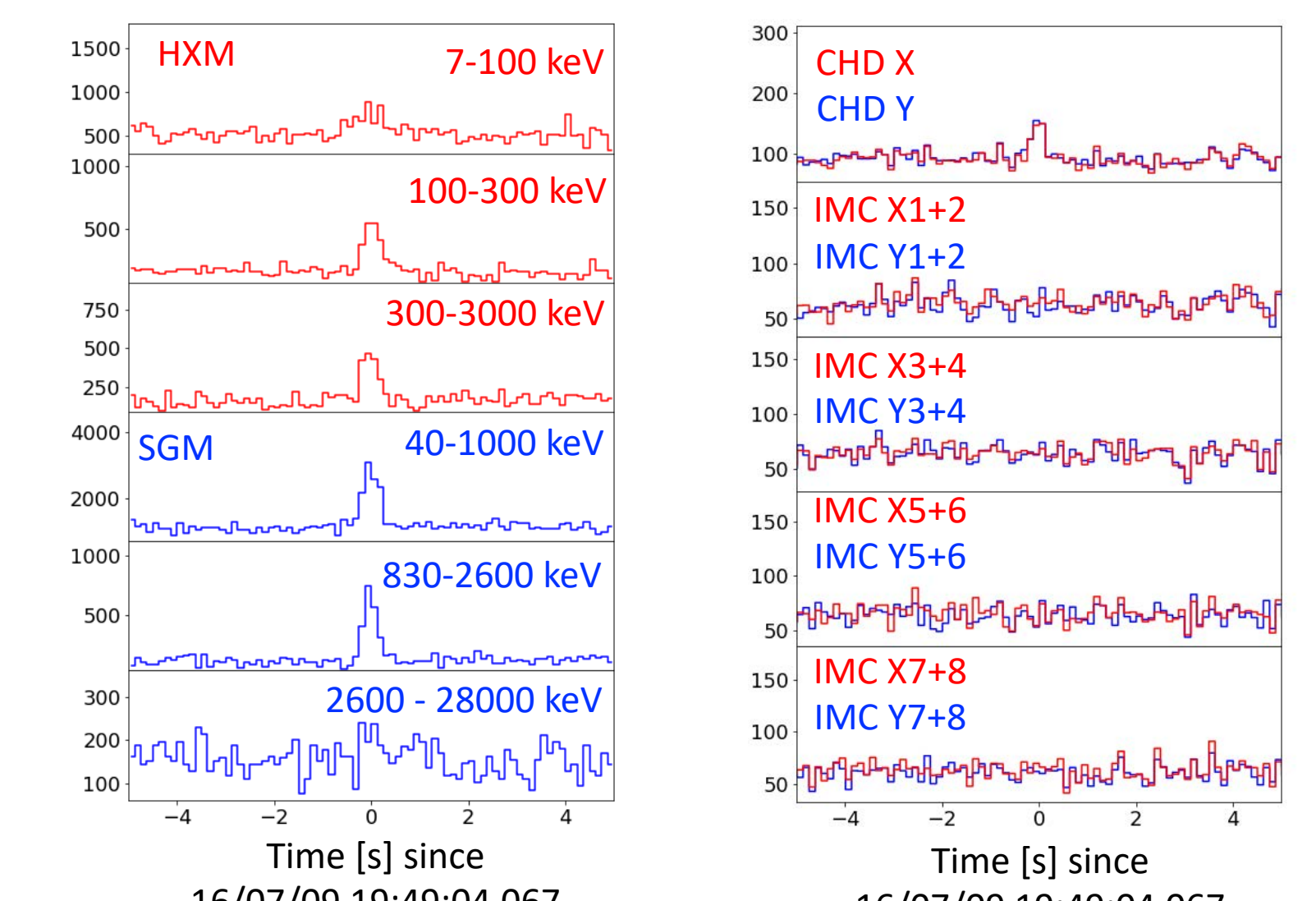


Figure 8. CGBM light curve and CHD & IMC count rates of GRB 160709A. CHD count rates increase around the time of CGBM detection.

References

- [1] Torii, *Proc. 35th ICRC*, 848, L13, 27, (2017).
- [2] Yamaoka, *Proc. 7th Huntsville Gamma-Ray Burst Symposium*, paper 41 in eConf Proceedings C1304143. (2013).
- [3] Abbott et al., *Phys Rev Lett*, 119, 161101, (2017)
- [4] Abbott et al., *ApJ Lett*, 848, L13, 27, (2017).

- [5] Band et al., *ApJ*, 413, 281, (1993)
- [6] Sari et al., *ApJ*, 497, L17, (1998)
- [7] The Gamma-ray Coordinates Network (GCN), <https://gcn.gsfc.nasa.gov/>
- [8] Goldstein et al., *ApJ Lett*, 848, L14, (2017).
- [9] Cannady et al., *in Proc. Sci (ICRC2019)*, in press (2019)

Acknowledgment

This work was supported by JAXA in Japan, NASA in U.S., and ASI in Italy. At LSU, support is provided by NASA grant NNX16AB99G.